Trellis-Based Baud-rate Timing Recovery Loop for Magnetic Recording Channels

Wei Zeng[‡], M. Fatih Erden[†], Aleksandar Kavčić[‡], Erozan M. Kurtas[†], Raman C. Venkataramani[†]

[‡] Division of Engineering and Applied Sciences, Harvard University, Cambridge, MA 02138

[†] Seagate Technology, Pittsburgh, PA 15222

***Abstract*— Timing recovery is crucial for magnetic recording systems. A conventional timing recovery loop (also known as the phase-locked loop) consists of a timing error detector (TED), a loop filter, and a voltage controlled oscillator (VCO), all of which process the samples in a sequential manner. This sequence of operations in the timing recovery loop performs well if the timing error is a small fraction of the bit interval. However, in the cycle-slip regions, the timing error is comparable to the bit interval, and the loop fails. In this paper, we represent the timing error in magnetic recording systems using a discrete Markov model that does not confine the timing error to only small fractions of the bit interval. By utilizing such a model, we derive an optimal baud-rate processing unit that does not perform tasks in sequence, but jointly. The derived unit has a similar structure as the classical first-order phase-locked loop (PLL). Simulation results show that the new detector outperforms the standard Mueller and Müller phase-locked loop. This performance gain is substantial if the timing error process is extremely noisy or if there is residual frequency-offset. For moderately low-noise timing errors without residual frequency-offset, the improvement over the Mueller and Müller phase-locked loop is just marginal.**

I. Introduction

Timing recovery is crucial to every communication and magnetic recording system, where the receiver needs to figure out the best instants at which to sample the received (or read-back) signal. In communication systems, the timing uncertainty may come from the slow drift of the receiver clock with respect to the transmitter clock. In magnetic recording systems, the mechanical motion fluctuation of the recording media during writing and reading processes will lead to timing uncertainty. The purpose of the timing recovery unit (or synchronizer) is to estimate such random timing uncertainty in order to adjust the sampler. This problem has been well studied in the literature and engineering practice, and several timing recovery schemes have been proposed. A comprehensive exposition and classification of these schemes can be found in [1],[2].

One of the most widely used digital decision-directed timing error detector (TED), which operates on the baud-rate samples of the baseband PAM signal, was proposed by Mueller and Müller [3](M&M). Adaptive Kalman filtering theory has been applied by Driessen [4] and Patapoutian [5] to a linearized baseband timing error model. A comprehensive analysis and comparison of several symbol-rate timing recovery schemes can be found in [6].

Another problem that is remarkably similar to the symbol timing recovery is the carrier phase recovery in communication systems that utilize carrier modulated signals. Many similar signal processing techniques can be applied here and have been thoroughly studied [7] [8]. Macchi and Scharf [9] derived a dynamic programming algorithm to jointly estimate the data sequence and phase error sequence, where the phase error sequence was modeled as an independent increment random process with modulo 2π. In [10], Dauwels and Loeliger studied the message passing algorithms for joint decoding and phase estimation over factor graphs. A key difference between phase error and timing error is that phase error only rotates the signal in the complex plane. However, timing error may cause symbol deletion or insertion (cycle-slip), which is much harder to correct. For example, a phase error of one period (2π) is equivalent to no phase error, while a timing error of one period means a cycle-slip.

Recently, new *iterative timing recovery* schemes were proposed for symbol detection in the presence of timing error. Such schemes utilize the power of iteratively decodable codes to combat the residual timing error (especially cycle-slips) after sampling. These iterative timing recovery schemes showed remarkable performance gains over the conventional detection schemes [11].

In this paper, we study timing recovery in the classical (i.e., non-iterative) setting, where the synchronization is performed by a *timing recovery loop*. Our goal is to design the optimal baud-rate timing recovery loop for baseband communication channels typical for magnetic recording systems. This is a rather difficult problem that has not been fully addressed in the past. Our solution is proposed for the timing error that can be modeled to be a discrete-time discrete-valued random process. This assumption is not precise in practice when the timing error is typically continuous-valued. However, by finely quantizing the continuous-valued timing error, we can closely approximate the continuous-valued random process and thus achieve an approximately optimal timing recovery loop.

Throughout the paper, uppercase letters denote random processes, while lowercase letters denote their realizations. The notation $P(\mathcal{E}_k = \varepsilon_k)$ denotes the probability of the event $\mathcal{E}_k = \varepsilon_k$. Similarly, $P(\mathcal{E}_k = \varepsilon_k | R_m = r_m)$ denotes the

[1]This work was supported by a grant from Seagate Technology.

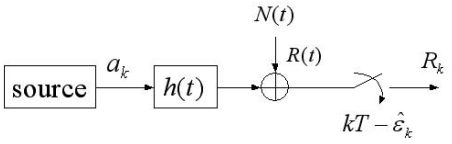

Fig. 1. A simple block diagram of the channel and signal model.

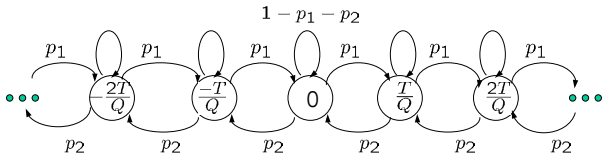

Fig. 2. The state transition diagram of the Markov timing error $\mathcal{E}_i$.

conditional probability. When no confusion can arise, we will use short notation $P(\varepsilon_k)$ and $P(\varepsilon_k|r_m)$ to denote $P(\mathcal{E}_k = \varepsilon_k)$ and $P(\mathcal{E}_k = \varepsilon_k|R_m = r_m)$ respectively. We will use ε_1^k to denote the vector $(\varepsilon_1, \ldots, \varepsilon_k)$.

II. Signal and Timing Error Model

We consider a simple system, as shown in Fig. 1. We denote the binary antipodal channel input symbol at time $k \in \mathbb{Z}$ by a_k ($a_k \in \{-1, 1\}$). The channel response function $h(t)$ is modulated by the channel input sequence $\{a_k\}$. The received waveform $R(t)$ is assumed to be of the following form

$$R(t) = \sum_k a_k h(t - kT) + N(t), \tag{1}$$

where T is the symbol interval and $N(t)$ is additive noise. To make the analysis simple, we assume that $\{a_k\}$ is a stationary, first order Markov process with transition probabilities

$$P(a_{k+1} = j|a_k = i) = \pi_{ij}, \quad i, j \in \{-1, 1\}. \tag{2}$$

If no timing error exist, the receiver will sample $R(t)$ at $t = iT$, for $i \in \mathbb{Z}$. However, if timing uncertainty exists, the real sampling instant will be $t = iT + \mathcal{E}_i$, where $\mathcal{E}_i$ represents the timing uncertainty of the i-th symbol, and is independent of the channel input $\{a_k\}$. We assume that the timing error $\mathcal{E}_i$ is a discrete-time, discrete-valued random process, that takes one of countably many values $\frac{jT}{Q}$, where j is an arbitrary integer and Q is the number of quantization levels in each symbol interval. We further assume that the timing error $\mathcal{E}_i$ can be represented by the following random walk process

$$\mathcal{E}_{i+1} = \mathcal{E}_i + \Delta_{i+1}, \tag{3}$$

$$P(\Delta_i = \delta_i) = \begin{cases} p_1 & \text{if } \delta_i = \frac{T}{Q} \\ p_2 & \text{if } \delta_i = -\frac{T}{Q} \\ 1 - p_1 - p_2 & \text{if } \delta_i = 0 \end{cases}. \tag{4}$$

The initial value is $\mathcal{E}_0 = 0$. The increments of the timing error, Δ_i, are assumed to be independent and identically distributed (i.i.d.) and are independent of input symbols and additive noise. Fig. 2 shows the state transition diagram of $\mathcal{E}_i$. When $E(\Delta_i) \neq 0$, i.e., $p_1 \neq p_2$, we have a system with residual frequency offset. If there is no residual frequency offset, we can simply let $p_1 = p_2$. More complicated Markov models can be adopted without changing the nature of the problem.

Our task in this paper will be to design the estimator that generates an estimate $\hat{\varepsilon}_i$ of $\mathcal{E}_i$. In that case, the receiver samples the received signal at time instants $iT + \mathcal{E}_i - \hat{\varepsilon}_i$. Denote the i-th sample at the receiver by R_i (with realization r_i),

$$R_i = \sum_k a_k h(iT - kT + \mathcal{E}_i - \hat{\varepsilon}_i) + N_i, \tag{5}$$

where N_i is the i-th sample of the noise. For simplicity, we shall assume that $N_i \sim \mathcal{N}(0, \sigma_N^2)$ are i.i.d. Gaussian noise. We shall use (5) as the sampled signal model in this paper.

III. Problem Formulation

A. Basic problem statement

The basic problem can be formulated as follows: upon receiving R_i, we need to make an estimate $\hat{\varepsilon}_{i+1}$ of the timing error $\mathcal{E}_{i+1}$. The value $\hat{\varepsilon}_{i+1}$ will be used to sample the received waveform at time instant $(i+1)T - \hat{\varepsilon}_{i+1}$.

Obviously, there are many choices of objective functions when designing the estimator for $\mathcal{E}_{i+1}$. In this section, we present one possible criterion. The method is based on maximum *a posteriori* probability (MAP) estimation given the observations R_1^i. Problem formulation is covered in detail in subsections III-C. However, before embarking on these detailed problem formulations, we introduce some more necessary notation.

B. More notation

Definition 1: [*residue timing error*] The residue timing error $\mathcal{T}_i$ (with realization τ_i) is defined as

$$\mathcal{T}_i = \mathcal{E}_i - \hat{\varepsilon}_i. \tag{6}$$

■

Definition 2: [*finite support function* $h(t)$] We assume that the channel response function $h(t)$ satisfies

$$h(t) = 0 \qquad \text{for } |t| \geq qT. \tag{7}$$

We denote the support interval of $h(t)$ by $(-qT, qT)$. ■

By using (6) and (7), We can now rewrite (5) as

$$R_i = \sum_{i-q+\lceil \tau_i/T \rceil}^{i+q+\lfloor \tau_i/T \rfloor} a_k h(iT - kT + \mathcal{T}_i) + N_i. \tag{8}$$

C. MAP estimation

In formulating the criterion for estimating $\mathcal{E}_{i+1}$, we take the advantage of the assumption that $\{\mathcal{E}_i\}$ is a slowly time-varying process. Thus, we can assign to $\hat{\varepsilon}_{i+1}$ the most likely value of $\mathcal{E}_i$ after observing r_1^i. That is

$$\begin{aligned} \hat{\varepsilon}_{i+1} &= \arg\max_{\varepsilon_i} P\left(\varepsilon_i | r_1^i, \hat{\varepsilon}_1^i\right) \\ &= \hat{\varepsilon}_i + \arg\max_{\tau_i} P\left(\tau_i | r_1^i, \hat{\varepsilon}_1^i\right) \\ &= \hat{\varepsilon}_i + \tilde{\tau}_i, \end{aligned} \tag{9}$$

where the second equality follows from (6). Notice that equation (9) is actually a first-order PLL, where $\arg\max_{\tau_i} P\left(\tau_i | r_1^i, \hat{\varepsilon}_1^i\right)$ defines a new TED. In Section IV, we give a recursive method for implementing the TED in (9).

This full text paper was peer reviewed at the direction of IEEE Communications Society subject matter experts for publication in the IEEE ICC 2006 proceedings.

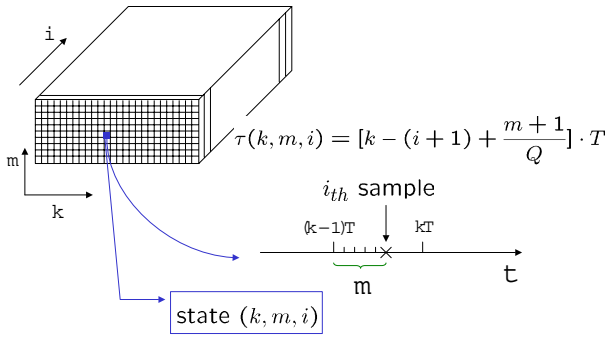

Fig. 3. Definition of the timing trellis states.

IV. Solution to the Single-Value-Based Estimation Problem

In this section, we illustrate how to compute the *a posteriori probability* in (9) recursively. Since both the timing error and the data sequence have memory, it is helpful to give a graphical interpretation of how the timing error and the data sequence propagate. We first define a timing trellis.

Timing error states: From our previous assumption (4), the sampling instants must fall on integer multiples of $\frac{T}{Q}$. Now, we partition the time axis into non-overlapping semi-open intervals $((k-1)T, kT]$, where $k \in \mathbb{Z}^+$. Each interval corresponds to a transmitted symbol. There are Q possible positions (quantization levels) where a sample can be taken within each interval.

We construct the timing trellis by representing each state (or, node) in the trellis with three variables (k, m, i). The physical interpretation of the state is: the i-th sample falls inside the k-th input interval $((k-1)T, kT]$ at the $(m+1)$-th quantization level, $m \in \{0, 1, \ldots, Q-1\}$, as illustrated in Fig.3. We observe that each state (k, m, i) is in a *1-to-1 correspondence* with the residue timing error τ_i for the i-th sample, i.e.,

$$\tau_i = \tau(k, m, i) = \left[k - (i+1) + \frac{m+1}{Q}\right] \cdot T, \tag{10}$$

where $m \in \{0, 1, \ldots, Q-1\}$. Conversely, for a given sample r_i, any value of τ_i also uniquely corresponds to a state (k, m, i).

Definition 3: [*the i-th plane*] We define those states (k, m, i) with the same index i as the i-th plane. Different states in the i-th plane are mapped to different values of τ_i. ■

We next need to figure out how the timing states propagate from the $(i-1)$-th (predecessor) plane to the i-th (successor) plane after the sample r_i is obtained. From (3), (6) and (9)

$$\begin{aligned} \mathcal{T}_i &= \mathcal{E}_i - \hat{\varepsilon}_i \\ &= \mathcal{E}_{i-1} + \Delta_i - (\hat{\varepsilon}_{i-1} + \tilde{\tau}_{i-1}) \\ &= \mathcal{T}_{i-1} + \Delta_i - \tilde{\tau}_{i-1}. \end{aligned} \tag{11}$$

Note that when the sample r_{i-1} is obtained, we can compute the estimated value $\tilde{\tau}_{i-1}$, so $\tilde{\tau}_{i-1}$ is regarded as a constant in (11). We observe two things from (11). First, starting from a given predecessor node in the $(i-1)$-th plane, we only go to three possible successor nodes in the i-th plane, corresponding to the three possible values of Δ_i, respectively, see (4). Second, the branches that link the states in the predecessor plane $i-1$ to the states in the successor plane i clearly depend on the value of $\tilde{\tau}_{i-1}$. Thus the state propagation is dynamically established at different steps i, after computing $\tilde{\tau}_{i-1}$.

Joint data and timing error states: In order to construct a graphical interpretation that can jointly represent the timing and data information, we expand our previous definition of the states in the timing trellis to a joint timing-data trellis.

From our finite-support assumption (7), at most

$$D = 2 \cdot q \tag{12}$$

data symbols are needed to calculate the value of each sample as shown by (8). They are $(a_{k-q}, \ldots, a_{k+q-1})$. To account for these D data symbols as well as the timing error, we expand the state variable m into a vector $(a_{k-q}, \ldots, a_{k+q-1}, m)$. Since $0 \le m < Q$, and $a_i \in \{-1, 1\}$ are binary integers, we can define a one-to-one mapping

$$(a_{k-q}, \ldots, a_{k+q-1}, m) \overset{1-to-1}{\longleftrightarrow} \bar{m}, \tag{13}$$

where

$$\bar{m} = m + Q \left[\sum_{j=k-q}^{k+q-1} 2^{k+q-1-j} \left(\frac{a_j + 1}{2}\right)\right]. \tag{14}$$

Thus in the new trellis, the state is defined as follows

Definition 4: [*Joint timing and ISI state*] A joint timing and ISI state is denoted by the tripple $s_i = (k, \bar{m}, i)$. ■

The full trellis then has the following properties: for each state (node) $s_i = (k, \bar{m}, i)$ in the full trellis, the timing state is captured by $m = (\bar{m} \bmod Q)$. Thus the corresponding residue timing error is

$$\begin{aligned} \tau_i &= \tau(s_i) = \tau(k, \bar{m}, i) \\ &= \left[k - (i+1) + \frac{(\bar{m} \bmod Q) + 1}{Q}\right] \cdot T. \end{aligned} \tag{15}$$

The ISI information of the state $(k, \bar{m}, i)$ is captured by

$$\sum_{j=k-q}^{k+q-1} 2^{k+q-1-j} \cdot \left(\frac{a_j + 1}{2}\right) = \left\lfloor \frac{\bar{m}}{Q} \right\rfloor. \tag{16}$$

Recursive state propagation: We consider the *a posteriori probability* in (9). From our previous definition of the state s_i, we get

$$\begin{aligned} P(\tau_i | r_1^i, \hat{\varepsilon}_1^i) &= \sum_{s_i : \tau(s_i) = \tau_i} P(s_i | r_1^i, \hat{\varepsilon}_1^i) \\ &= \sum_{s_i : \tau(s_i) = \tau_i} \left[\sum_{s_1^{i-1}} P(s_1^i | r_1^i, \hat{\varepsilon}_1^i)\right]. \end{aligned} \tag{17}$$

We next manipulate the term on the right-hand side of (17) to derive a recursive formula. Using the Bayes rule, we have

$$P\left(s_1^i | r_1^i, \hat{\varepsilon}_1^i\right) = C \cdot \gamma(s_{i-1}, s_i, r_i) \cdot P(s_1^{i-1} | r_1^{i-1}, \hat{\varepsilon}_1^{i-1}), \tag{18}$$

This full text paper was peer reviewed at the direction of IEEE Communications Society subject matter experts for publication in the IEEE ICC 2006 proceedings.

where

$$\gamma(s_{i-1}, s_i, r_i) = P(r_i|s_i) \cdot P(s_i|s_{i-1}), \quad (19)$$

$$C = \frac{P(r_1^{i-1}, \hat{\varepsilon}_1^{i-1})}{P(r_1^i, \hat{\varepsilon}_1^i)}. \quad (20)$$

(Proof provided in appendix.) Now the summation within the brackets in (17) can be derived recursively by using (18),

$$\begin{aligned} &\sum_{s_1^{i-1}} P(s_1^i|r_1^i, \hat{\varepsilon}_1^i) \quad (21)\\ &= C \cdot \gamma(s_{i-1}, s_i, r_i) \sum_{s_1^{i-1}} P(s_1^{i-1}|r_1^{i-1}, \hat{\varepsilon}_1^{i-1}) \\ &= C \sum_{s_{i-1}} \gamma(s_{i-1}, s_i, r_i) \left[\sum_{s_1^{i-2}} P(s_1^{i-1}|r_1^{i-1}, \hat{\varepsilon}_1^{i-1}) \right]. \end{aligned}$$

We notice that C does not depend on the states and can be viewed as a constant at the i-th step. We therefore ignore this constant and introduce the following recursive *accumulated metric* definition based on (21).

Definition 5: [*accumulated metric* $c'(s_i)$] We define the metric $c'(s_i)$ of an arbitrary state $s_i \in \{(k_i, \bar{m}_i, i)\}$ in the i-th plane as

$$c'(s_i) \stackrel{\triangle}{=} \sum_{s_{i-1}} \gamma(s_{i-1}, s_i, r_i) \cdot c'(s_{i-1}), \quad (22)$$

with the initial condition

$$c'(s_0) = \begin{cases} 1, & \text{if } s_0 = (0, Q-1, 0), \\ 0, & \text{otherwise} \end{cases}. \quad (23)$$

The function $\gamma(s_{i-1}, s_i, r_i)$ is computed according to (19).■

Based on the above definition and the result in (17), the estimation rule given by (9) is equivalent to

$$\hat{\varepsilon}_{i+1} = \hat{\varepsilon}_i + \arg\max_{\tau_i} \sum_{s_i:\tau(s_i)=\tau_i} c'(s_i). \quad (24)$$

Recursive state propagation algorithm: We now formulate a state propagation algorithm for timing recovery.

1) The system is assumed to be perfectly synchronized at time $i = 0$ (i.e., $\varepsilon_0 = 0$), and we assume $a_k = 0$ for $k < q$. The initial condition of our algorithm is (23). In practice, this assumption is satisfied by using preambles. (Initialization with non-perfect synchronization at time $i = 0$ is also possible.)
2) Whenever the loop detector receives the i-th sample r_i, for $i \geq 1$, we calculate all the state metrics $c'(s_i)$ in the i-th plane according to (22). Normalize the states such that $\sum c'(s_i) = 1$.
3) The next-step timing error estimate $\hat{\varepsilon}_{i+1}$ is computed by (24).
4) For all states s_{i-1}, delete $c'(s_{i-1})$ from the memory.
5) Use $\hat{\varepsilon}_{i+1}$ to take the $(i+1)$-th sample, go to step 2.

Complexity and memory cost: We notice that the state propagation in the above algorithm is similar as the forward recursion of the Bahl-Cocke-Jelinek-Raviv (BCJR) algorithm [12]. However, since we *do not need backward recursions* to make the decision, previous state metrics are always deleted from the memory in step 4. Therefore, the memory cost in the proposed algorithm does not grow with block length n. On the other hand, it is not necessary to evaluate all the state metrics $c(s_i)$ of the i-th plane in step 2. In practice, if we assume that the timing error estimate is not too bad, i.e., $|\tau_i| \leq dT$ for $1 \leq i \leq \ell$, and $d \in \mathbb{Z}^+$ is a fixed integer, we only need to consider those states $s_i = (k, \bar{m}, i)$ such that $|k - i| \leq d$. Simulation results show that for most cases, it is sufficient to choose $d = 2$ without any loss in performance. The amount of memory, i.e., the number of state metrics, required for the proposed algorithm is $2d \cdot Q \cdot 2^{2q}$. Therefore, the computational complexity (the number of multiplications and additions) at each step is also proportional to $d \cdot Q \cdot 2^{2q}$.

V. Simulation Results

To assess the quality of the derived timing recovery method, the algorithm in Sections IV is compared to the conventional timing recovery loop as well as to the perfect timing scenario. The i.i.d. data symbols are generated by equiprobable binary source, and are first passed through filter $G(D) = 1 - D^2$, as shown by Fig.4. We assume that $h(t)$ is a truncated $sinc$ function with the form $h(t) = \text{sinc}(\frac{t}{T})\,[u(t+T) - u(t-T)]$, where $u(t)$ is the unit step function. If there is no timing error, the channel is equivalent to the $PR4$ channel. To make the system more realistic, the real timing error $\{\mathcal{E}_i\}$injected into the channel (5) during the simulation is a Gaussian independent increment process $\mathcal{E}_i = \mathcal{E}_{i-1} + W_i$, where $W_i \sim \mathcal{N}(\mu_w T, \sigma_w^2 T^2)$ are i.i.d. Gaussian random variables. Therefore this timing error process has a frequency offset

$$\Delta f_1 = \frac{1}{T + \mu_w} - \frac{1}{T}.$$

For the purpose of designing the loop detector for this timing error, we approximate the timing error by the model in (3) and (4). This discrete model has a frequency offset

$$\Delta f_2 = \frac{1}{T + \frac{T}{Q}(p_1 - p_2)} - \frac{1}{T}.$$

In practice, the parameters p_1 and p_2 can be iteratively estimated from the received signal using the Baum-Welch algorithm [13]. (Note that we could use a more sophisticated Markov timing model, but it suffices to use the simple one in (3) and (4) to illustrate the principle.) The final *residual* frequency offset of the system is

$$\begin{aligned} \Delta f &= \Delta f_1 - \Delta f_2 \\ &= \frac{1}{T + \mu_w} - \frac{1}{T + \frac{T}{Q}(p_1 - p_2)} \\ &\approx -\frac{1}{T}\left(\frac{\mu_w}{T} - \frac{p_1 - p_2}{Q}\right). \end{aligned} \quad (25)$$

This full text paper was peer reviewed at the direction of IEEE Communications Society subject matter experts for publication in the IEEE ICC 2006 proceedings.

This approximation is based on the assumption that $|\mu_w| \ll T$ and $\left|\frac{p_1-p_2}{Q}\right| \ll 1$. In the following simulations, we set $T = 1$ and $p_1 = p_2$. Since the method operates on baud-rate, we compare it with the standard phase-locked loop (PLL) using the Mueller and Müller (M&M) detector [3] for systems with and without residual frequency-offset.

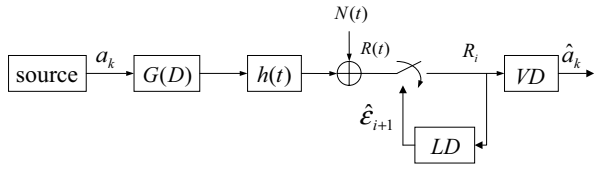

Fig. 4. The un-coded system used in simulation. LD represents the loop detector. VD represents the Viterbi detector for data detection.

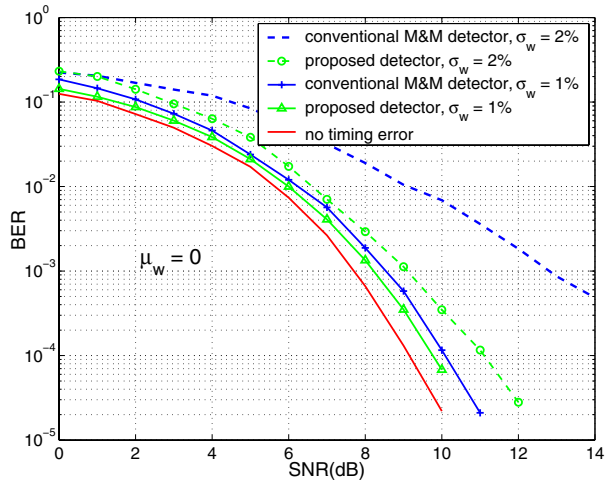

Fig. 5. Bit error rate (BER) performance using the recursive detector. Timing error increments are i.i.d Gaussian random variables with zero-mean.

Fig.5 compares the bit error rate (BER) performance of the recursive timing error detector when there is no residual frequency-offset, i.e., $\mu_w = 0$ and $p_1 = p_2$, to the standard first-order PLL with the M&M detector. The filter coefficients in the standard PLL were exhaustively optimized for every SNR respectively. The quantization level for the proposed recursive detector is fixed to $Q = 10$. We observe that for $\sigma_w = 0.01$, the proposed recursive detector only provides marginal performance gain over the optimum M&M detector. However, as the timing error increases to $\sigma_w = 0.02$, there is large performance gains attained by the new detector in all SNR regions.

Fig.6 compares the BER performance of the recursive timing error detector when there is residual frequency-offset, i.e., $\Delta f \neq 0$, to the standard second-order PLL with the M&M detector. The parameters of the timing error increment is set to $\sigma_w = 0.01$ and $\mu_w = 0.5\%$. Both filter coefficients in the M&M detector, as well as the delay length of the Viterbi detector before the M&M detector were exhaustively optimized for each SNR, respectively. We observe that the proposed recursive detector is not very sensitive to the frequency-offset,

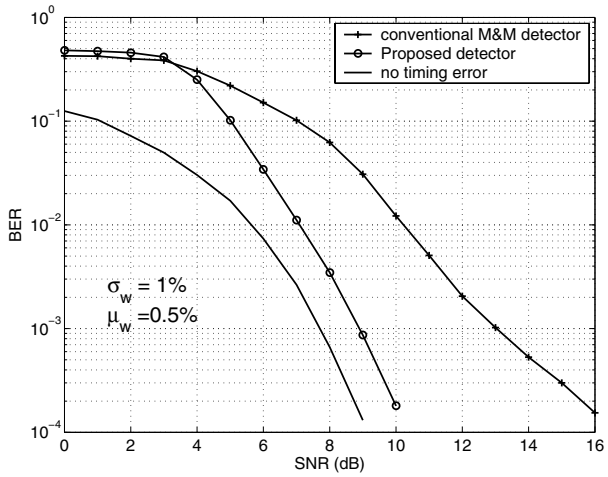

Fig. 6. Bit error rate (BER) performance using the recursive detector. Timing error increments are i.i.d Gaussian random variables with nonzero-mean.

and provides large performance gain over the conventional PLL. Block by block simulation results show that probability of having cycle-slip, where large burst of detection errors occur, is greatly reduced by using the recursive timing error detector. Fig.7 compares the probability of cycle-slip of the proposed timing recovery loop to the second-order PLL with M&M detector.

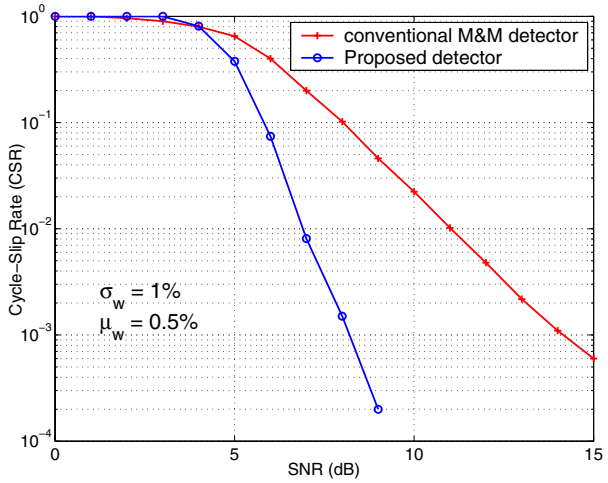

Fig. 7. Cycle-slip rate performance using the recursive detector. Timing error increments are i.i.d Gaussian random variables with nonzero-mean.

VI. Conclusion

In this work, we proposed an optimization criterion for timing error estimation, and derived a recursive timing recovery algorithm, under the assumption that the timing error can be modeled as a discrete Markov chain. We compared the bit error rate performance of the newly derived detector to the conventional timing recovery loop (with a Mueller and Müller detector), and observed an obvious performance gain when the timing error is large or when there is residual

This full text paper was peer reviewed at the direction of IEEE Communications Society subject matter experts for publication in the IEEE ICC 2006 proceedings.

frequency-offset. For low-timing-error systems without residual frequency-offset, the traditional phase-locked loop with a Mueller and Müller detector works just as well. These results are obtained for un-coded system only. The usage of such a detector in coded systems can be studied in future.

APPENDIX

In this appendix, we prove eqn. (18).

Proof: By using the Bayes rule, we have

$$\begin{aligned} P\left(s_1^i|r_1^i,\hat{\varepsilon}_1^i\right) &= P\left(s_1^i,r_1^i,\hat{\varepsilon}_1^i\right)/P\left(r_1^i,\hat{\varepsilon}_1^i\right) \\ &= P\left(s_1^{i-1}|r_1^{i-1},\hat{\varepsilon}_1^{i-1}\right)\frac{P(r_1^{i-1},\hat{\varepsilon}_1^{i-1})}{P(r_1^i,\hat{\varepsilon}_1^i)} \\ &\quad \cdot P\left(s_i,r_i|s_1^{i-1},r_1^{i-1},\hat{\varepsilon}_1^{i-1}\right). \end{aligned} \tag{26}$$

The last term in (26) can be further simplified as

$$\begin{aligned} &P\left(s_i,r_i|s_1^{i-1},r_1^{i-1},\hat{\varepsilon}_1^{i-1}\right) \\ &\quad = P\left(s_i|s_1^{i-1},r_1^{i-1},\hat{\varepsilon}_1^{i-1}\right)\cdot P\left(r_i|s_1^i,r_1^{i-1},\hat{\varepsilon}_1^{i-1}\right). \end{aligned} \tag{27}$$

Since s_i contains both the timing and ISI information for the i-th sample r_i, we have

$$P(r_i|s_1^i,r_1^{i-1},\hat{\varepsilon}_1^{i-1}) = P(r_i|s_i). \tag{28}$$

Next by using the one-to-one correspondense between the state s_i on one side and the timing error and ISI information as a pair on the other, we have

$$\begin{aligned} &P\left(s_i|s_1^{i-1},r_1^{i-1},\hat{\varepsilon}_1^{i-1}\right) \\ &\quad = P\left(\tau_i,a_{\ell(i)-D+1}^{\ell(i)}|\tau_1^{i-1},a_1^{\ell(i-1)},r_1^{i-1},\hat{\varepsilon}_1^{i-1}\right) \\ &\quad \overset{(h)}{=} P\left(\tau_i|\tau_{i-1},\hat{\varepsilon}_{i-1}^i\right)\cdot P\left(a_{\ell(i-1)+1}^{\ell(i)}|a_{\ell(i)}\right) \qquad (29) \\ &\quad \overset{(i)}{=} P(s_i|s_{i-1}), \qquad (30) \end{aligned}$$

where (h) follows from the Markovian assumption, and (i) is based on the observation that s_{i-1} actually contains all the information in the conditioning. By substituting (27), (28), and (30) into (26), we obtain the recursive formula (18). ■

REFERENCES

[1] H. Meyr, M. Moeneclaey, and S. A. Fechtel, *Digital Communication Receivers*. New York, USA: Wiley & Sons, 1998.

[2] L. E. Franks, "Carrier and bit synchronization in data communication – a tutorial review," *IEEE Trans. Communications*, vol. 28, no. 8, pp. 1107–1121, August 1980.

[3] K. H. Mueller and M. Müller, "Timing recovery in digital synchronous data receivers," *IEEE Trans. Communications*, vol. 24, no. 5, pp. 516–531, May 1976.

[4] P. F. Driessen, "DPLL bit synchronizer with rapid acquisition using adaptive kalman filtering techniques," *IEEE Trans. Communications*, vol. 42, no. 9, pp. 2673–2675, September 1994.

[5] A. Patapoutian, "On phase-locked loops and Kalman filters," *IEEE Trans. Communications*, vol. 47, no. 5, pp. 670–672, May 1999.

[6] P. M. Aziz and S. Surendran, "Symbol rate timing recovery for higher order partial response channels," *IEEE Journal on Selected Areas in Communications*, vol. 19, no. 4, pp. 635–648, April 2001.

[7] W. C. Lindsey and M. K. Simon, *Telecommunication Systems Engineering*. Eaglewood cliffs, USA: Prentice Hall, 1973.

[8] J. G. Proakis, *Digital Communications*. USA: McGraw Hill, 2001.

[9] O. Macchi and L. L. Scharf, "A dynamic programming algorithm for phase estimation and data decoding on random phase channels," *IEEE Trans. Information Theory*, vol. 27, no. 5, pp. 581–595, Semptember 1981.

[10] J. Dauwels and H.-A. Loeliger, "Joint decoding and phase estimation: an exercise in factor graphs," in *Proc. of the IEEE International Symposium on Information Theory*, Yokohama, Japan, June 2003, p. 231.

[11] J. R. Barry, A. Kavčić, S. W. McLaughlin, A. Nayak, and W. Zeng, "Iterative timing recovery," *IEEE Signal Processing Magazine*, vol. 21, no. 1, pp. 89–102, January 2004.

[12] L. R. Bahl, J. Cocke, F. Jelinek, and J. Raviv, "Optimal decoding of linear codes for minimizing symbol error rate," *IEEE Trans. Information Theory*, vol. 20, pp. 284–287, March 1974.

[13] W. Zeng, R. Motwani, and A. Kavčić, "Estimation of the timing error process parameters using the Baum-Welch algorithm," presented at the Magnetic Recording Conference, Stanford, CA, August 15-17, 2005.

This full text paper was peer reviewed at the direction of IEEE Communications Society subject matter experts for publication in the IEEE ICC 2006 proceedings.